# Cool-edge populations of the kelp Ecklonia radiata under global ocean change scenarios

Britton, Damon; Layton, Cayne; Mundy, Craig N.; Brewer, Elizabeth A.; Gaitán-Espitia, Juan Diego; Beardall, John

*Published in:*
Proceedings of the Royal Society B: Biological Sciences

*DOI:*
10.1098/rspb.2023.2253

*Publication date:*
2024

PROCEEDINGS B

royalsocietypublishing.org/journal/rspb

Research

**Cite this article:** Britton D, Layton C, Mundy CN, Brewer EA, Gaitán-Espitia JD, Beardall J, Raven JA, Hurd CL. 2024 Cool-edge populations of the kelp *Ecklonia radiata* under global ocean change scenarios: strong sensitivity to ocean warming but little effect of ocean acidification. *Proc. R. Soc. B* **291**: 20232253.
https://doi.org/10.1098/rspb.2023.2253

Received: 4 October 2023
Accepted: 4 December 2023

**Subject Category:**
Global change and conservation

**Subject Areas:**
physiology, ecology, plant science

**Keywords:**
physiology, phenotypic plasticity, ocean warming, ocean acidification, thermal performance curves, multiple drivers

**Author for correspondence:**
Damon Britton
e-mail: damon.britton@utas.edu.au

Electronic supplementary material is available online at https://doi.org/10.6084/m9.figshare.c.6991797.

THE ROYAL SOCIETY PUBLISHING



# Cool-edge populations of the kelp *Ecklonia radiata* under global ocean change scenarios: strong sensitivity to ocean warming but little effect of ocean acidification

Damon Britton[1], Cayne Layton[1], Craig N. Mundy[1], Elizabeth A. Brewer[2], Juan Diego Gaitán-Espitia[3], John Beardall[4], John A. Raven[5,6,7] and Catriona L. Hurd[1]

[1]Institute for Marine and Antarctic Studies, University of Tasmania, 20 Castray Esplanade, Battery Point, Hobart, Tasmania 7004, Australia
[2]CSIRO Oceans and Atmosphere, Hobart, Tasmania 7000, Australia
[3]School of Biological Sciences and the SWIRE Institute of Marine Sciences, The University of Hong-Kong, Hong Kong, People's Republic of China
[4]School of Biological Sciences, Monash University, Clayton, Victoria 3800, Australia
[5]Division of Plant Science, University of Dundee at the James Hutton Institute, Invergowrie, Dundee DD2 5DA, UK
[6]School of Biological Sciences, University of Western Australia, 35 Stirling Highway, Crawley, Western Australia 6009, Australia
[7]Climate Change Cluster, University of Technology, Sydney, Ultimo, New South Wales 2007, Australia

DB, 0000-0002-9029-7527; CL, 0000-0002-3390-6437; JDG-E, 0000-0001-8781-5736

Kelp forests are threatened by ocean warming, yet effects of co-occurring drivers such as $CO_2$ are rarely considered when predicting their performance in the future. In Australia, the kelp *Ecklonia radiata* forms extensive forests across seawater temperatures of approximately 7–26°C. Cool-edge populations are typically considered more thermally tolerant than their warm-edge counterparts but this ignores the possibility of local adaptation. Moreover, it is unknown whether elevated $CO_2$ can mitigate negative effects of warming. To identify whether elevated $CO_2$ could improve thermal performance of a cool-edge population of *E. radiata*, we constructed thermal performance curves for growth and photosynthesis, under both current and elevated $CO_2$ (approx. 400 and 1000 µatm). We then modelled annual performance under warming scenarios to highlight thermal susceptibility. Elevated $CO_2$ had minimal effect on growth but increased photosynthesis around the thermal optimum. Thermal optima were approximately 16°C for growth and approximately 18°C for photosynthesis, and modelled performance indicated cool-edge populations may be vulnerable in the future. Our findings demonstrate that elevated $CO_2$ is unlikely to offset negative effects of ocean warming on the kelp *E. radiata* and highlight the potential susceptibility of cool-edge populations to ocean warming.

## 1. Introduction

Anthropogenic climate change is having unprecedented effects on the oceans, with rising temperatures and elevated $CO_2$ concentrations having adverse impacts on nearly all marine ecosystems [1]. Of particular concern, is declines in a range of habitat forming species such as kelps (order Laminariales, [2,3]), which support diverse and productive ecosystems in temperate and subpolar regions globally [4,5]. Substantial research effort has been undertaken in the last 10–15 years to identify kelp species and communities that are vulnerable to

global ocean change [3,6,7]. However, there remain significant gaps in our understanding of the combined effect of multiple co-occurring drivers such as temperature and $CO_2$ [8,9]. Identifying key interactions between major components of global ocean change such as elevated temperature and dissolved $CO_2$ and identifying the threshold at which a driver such as temperature becomes a stressor is urgently required to improve our ability to accurately predict changes and identify vulnerable species and communities.

Since 1850, the surface of the ocean has warmed by approximately 1°C, with a further 2–3°C increase projected by the end of the century depending on which emissions scenario is realized (ocean warming, [1]). Many kelps are highly sensitive to thermal stress as evidenced by the declines and local extinctions associated with ocean warming [3,6,10] and extreme and acute warming events (i.e. marine heatwaves; [11–13]). Further losses of kelp have been projected throughout the twenty-first century [14]. For example, modelling work by Martínez *et al*. [14] suggests up to 70–100% declines in the distrubution of multiple Australian kelps and prominent fuciods by 2100. However, much research has focused on populations at the warm edge of a species' range (e.g. [12,15]), which are already experiencing thermal stress. Often overlooked, however, are populations from cooler edges of species' ranges, which are thought to be more tolerant to ocean warming as they exist below the thermal optima of the species. As such, our knowledge of intraspecific variation in thermal tolerance and the wider impact of ocean warming across species ranges remains limited [16,17]. This is problematic as, by assuming warm-edge populations are more susceptible, we may consider that range contractions under climate change will be linear and ignore the susceptibility of populations adapted to cooler waters [18]. There is growing evidence that the thermal tolerances of populations from different thermal regimes differ due to local adaptation for kelps [18,19], corals [20,21] and invertebrates [22,23]. Identifying whether these cool-edge populations are equally susceptible is therefore key to providing a better understanding of how a species as a whole will respond to ocean warming.

One way to improve our understanding of kelps' vulnerability to ocean warming is to generate population-level thermal performance curves (TPCs, [24,25]). TPCs describe the relationship between a physiological process (e.g. photosynthesis or growth) over a wide range of temperatures. Physiological performance (referred to hereafter as performance unless stated otherwise), as a function of temperature, can then also be used to model a species response to changing temperatures. This can lead to an improved understanding of a species performance over yearly cycles, identify potential sub-lethal effects, and periods of highest susceptibility to extreme warming events. However, performance is not only influenced by temperature but also by the interactions of other environmental drivers, which are often overlooked in projections of how kelps will respond to climate change [14]. Understanding the interactive effects of co-occurring drivers, such as dissolved $CO_2$ and temperature, is urgently required, as responses across taxa can be varied. For example, both algal turfs and seagrass display enhanced thermal tolerance under elevated $CO_2$ [26,27], whereas the two drivers can act synergistically to reduce performance in crustaceans [28]. Identifying the nature of these interactions for foundation species such as kelps is critical for improving the reliability and accuracy of predictions of how species will respond to global ocean change.

The sustained absorption of atmospheric $CO_2$ has led to an increase in the dissolved $CO_2$ concentrations of the surface ocean of approximately 70% and subsequent changes to the seawater carbonate system (ocean acidification, [1]). By 2100, dissolved $CO_2$ levels are projected to be approximately 150–200% higher than in 1850 depending on which emissions scenario is realized [1]. As $CO_2$ is required for photosynthesis, elevated $CO_2$ concentrations are likely to have vastly different effects to that of ocean warming [29,30]. It is unlikely that kelps are carbon limited under today's $CO_2$ concentrations, as they possess a carbon dioxide concentrating mechanism (CCM). CCMs increase the kelp's affinity for inorganic carbon by increasing $CO_2$ concentrations at the active site of Rubisco, ensuring photosynthesis is essentially $CO_2$-saturated under present-day concentrations [31,32]. As such, the idea that $CO_2$ will have a 'fertilizer effect' and directly increase productivity of kelps is unlikely [30,33]. However, if kelps can downregulate the CCM to rely more on diffusive uptake of $CO_2$ as an inorganic carbon source, then this may endow an energetic saving via a reduced need to operate CCMs, which could be used to enhance growth or acclimatize to elevated temperatures [34]. Energetic savings arising from CCM downregulation has been proposed as a way in which the habitat forming fucoid *Phyllospora comosa* is able to tolerate elevated temperatures [34]. The proposed mechanism suggests that energetic savings arising from CCM downregulation are used to alter cellular membrane fatty acid composition, which in turn reduce the negative effects of increased membrane fluidity at high temperatures [34]. A similar mechanism occurs in response to elevated inorganic nitrogen conditions in the kelp *Macrocystis pyrifera* (giant kelp), where adjustments in fatty acid composition increases thermal optima [35,36]. Elevated $CO_2$ has been shown to enhance performance at elevated temperatures in algal turfs [26], seagrass [27] and terrestrial plants [37], suggesting this may be a widespread phenomenon; however, it requires further investigation in kelps.

In Australia, kelp forests form the foundation of the Great Southern Reef, a continental-scale temperate rocky reef system which is a global hotspot for marine biodiversity and endemism [19]. The region is also an ocean warming hotspot, with both the waters of southeast and southwest of Australia warming at rates of three to four times the global average [38]. This warming has already been linked to approximately 95% declines in the canopy cover of *M. pyrifera* forests in Tasmania, southeastern Australia, since the 1970s [10,39]. The most abundant and widespread kelp across the broader Great Southern Reef is *Ecklonia radiata* (C.Agardh) J.Agardh, which has a widespread distribution from subtropical latitudes (approx. 27° N) on both east and west coasts of Australia, to the cold temperature regions in southern Tasmania (approx. 44° S, [40]). The species can survive temperatures as high as 28°C, and the optimum temperature for net photosynthesis of *E. radiata* sporophytes in Western Australia is 24°C [15]. Moreover, the gametophyte life stage displays evidence of acclimatization or adaptation to local thermal regimes, with higher thermal optima positively correlated with higher *in situ* temperatures [41]. Recent modelling work by Young *et al*. [42] demonstrated the potential for declines in *E. radiata* cover in cool-edge populations of the southeastern Australian state of Victoria, with one of the

main drivers being increased sea surface temperatures. However, there is little understanding of the thermal tolerance of *E. radiata* sporophytes at the physiological level from populations at the cool edge of its distribution, and no studies have assessed whether thermal performance is likely to change with the elevated levels of $CO_2$ projected under global ocean change. Accordingly, the aims of this study were threefold: (i) identify the thermal optima for growth and photosynthesis for cool-edge populations of *E. radiata* in Australia, (ii) examine whether thermal performance of growth and photosynthesis changes under elevated $CO_2$, and (iii) use these modelled relationships to identify timepoints in which performance of this cool-edge population of *E. radiata* will decline under global ocean change scenarios. The results of this study highlight a previously unrecognized susceptibility of cool-edge populations of *E. radiata* to ocean warming, which is unlikely to be mitigated by ocean acidification.

## 2. Material and methods

### (a) Collection and acclimatization

Approximately 100 individual juvenile *E. radiata* sporophytes of approximately 10 cm length were collected on 2 February 2021 from Coal Point, Tasmania (43.33430° S, 147.32493° E) from 6–8 m depth by divers on SCUBA. Individuals were placed in an insulated container in darkness in seawater following collection and transported back to the laboratory approximately 2 h away. Once in the laboratory, all individuals were acclimatized to laboratory conditions by placement in a common 40 l container containing filtered seawater (0.2 µm pore size) in a temperature-controlled room set at 16°C, this was similar to the field site which had an average sea surface temperature (SST) in preceding 14 days of 17.87°C [43]. Lighting was provided by dimmable LED lights (Zeus-70, Ledzeal, Hong Kong), that mimicked the colour spectrum present at approximately 8 m water depth on a 12 : 12 light dark cycle. Mean irradiance was 70 µmol $m^{-2}$ $s^{-1}$; however, this varied over the day to mimic a natural light cycle, increasing linearly from 0 to 130 µmol $m^{-2}$ $s^{-1}$ between 06.00 and 11.00, and then maintained at 0–130 µmol $m^{-2}$ $s^{-1}$ until 13.00 when it then decreased linearly again back to 0 µmol $m^{-2}$ $s^{-1}$ at 18.00. Individuals were kept under these conditions for 72 h.

### (b) Experimental culture conditions

Following laboratory acclimatization, 80 individuals were haphazardly allocated to one of eight 15 l containers, filled with filtered and aerated seawater at ambient $CO_2$ levels. The temperature of each container was then increased/decreased to the experimental temperature (6, 9, 12, 16, 20, 23, 26 and 29°C) at a rate of 2°C per day. When each bath reached its target experimental temperature (0–6.5 days depending on the treatment), those individuals were each attached to a small pebble (approx. 30 mm ∅) by their holdfast using a rubber band, and haphazardly allocated to one of 10 2 l experimental chambers. Within each temperature treatment, half of the chambers were maintained at ambient $pCO_2$ (target 420 µatm) and the other half at the future $pCO_2$ (target 1000 µatm, simulating the upper projections of representative concentration pathway (RCP) 8.5, [1]) level giving a total of five replicates ($n = 5$) for each of the 16 unique combinations of temperature and $CO_2$ ($N = 80$). For each treatment, the experiment was considered to have begun at this point, therefore the starting date for each treatment was staggered depending on the time to reach the target temperature. Each treatment ended after 21 days at the experimental temperature.

The experiment took place within the same temperature-controlled room as the laboratory acclimatization, which was set at 16°C. Temperature treatments were maintained using water baths that were modified using either chiller units (6, 9, 12°C; RC1, Ratek Instruments and C2G, Grant Instruments) or heaters (20, 23, 26 and 29°C; T100, Grant Instruments and Aqua One IPX8, Kongs Australia) all via independent temperature-controller units (T100, Grant Instruments and Temperature Controller 7028/3, Tunze). The 16°C water bath remained at the ambient temperature of the temperature-controlled room. Temperatures in each bath were monitored and recorded using temperature loggers (HOBO Pendant MX Temp, Onset Computer Corporation). Water in each experimental chamber was replaced every 3–4 days for the duration of the acclimatization and experiment to allow replenishment of seawater nutrient concentrations depleted by the kelp. Water samples for determination of nitrate and ammonium concentrations were taken in a subset of chambers just prior to the final water change of the experiment. Samples were filtered to 0.7 µm (GF/F, Whatman) and immediately frozen at −20°C in 12 ml polyethylene vials. Samples were subsequently thawed, and ammonium and nitrate concentrations were determined using a QuickChem 8000 Automated Ion Analyser (LaChat Instruments).

The two $pCO_2$ treatments were maintained by constant bubbling of each chamber with either air (for ambient $pCO_2$) or an elevated $CO_2$/air mix (for future $pCO_2$). Filtered air was provided by outlets in the temperature control room sourced within the building and $CO_2$ provided by a single $CO_2$ cylinder ($CO_2$ food grade, BOC Gas and Gear). Elevated $CO_2$/air mixes were controlled by adjusting the voltage on mass flow controllers (FMA5418A and FMA5402A, Omega Engineering). These voltages were maintained for the duration of the experiment to ensure constant delivery of the same $pCO_2$ to the enriched chambers. $CO_2$ levels were not increased slowly, as for temperature, as pilot studies and previous experiments indicated no adverse effects of instantaneously adding elevated $CO_2$. All experimental chambers had a small outlet to allow the bubbled gas to escape from the otherwise sealed container. To monitor the concentration of dissolved inorganic carbon (DIC), pH was monitored daily using a spectrophotometric pH system [46] in randomized chambers from each of the 16 unique combinations of temperature and $pCO_2$ daily until the end of the first treatment on 25 February 2021. Samples of seawater for determination of total alkalinity were taken from a random chamber within each of the 16 unique experimental combinations (two samples per combination) on 19 February 2021. Samples (approx. 60 ml) were filtered to 0.2 µm and immediately poisoned with $HgCl_2$ (0.02% v/v) until later analysis. Total alkalinity was analysed using a total alkalinity titrator (862 Compact Titrosampler, Metrohm) using best practice methods [47]. DIC and $pCO_2$ were calculated in CO2SYS [48] using the constants of Mehrbach *et al.* [49] refit by Lueker *et al.* [50] and the known $A_T$, pH, temperature and salinity (measured with an Orion Versa Star Advanced Electrochemistry Meter, ThermoFisher Scientific) of the seawater.

### (c) Biotic responses

#### (i) Growth (linear extension) and change in wet weight (%)

Growth was measured to provide information on the capacity of the kelp to increase biomass, and change in wet weight provided a holistic measure of growth (increase in biomass) minus tissue loss (erosion). To measure rates of linear extension, a single 5 mm diameter hole was punched in the blade of each individual above the meristem prior to photographing on day 1 [51]. Photographs were again taken at the end of the experiment on day 21 and the distance of the hole from the base of the blade was calculated using the software Fiji [52]. Linear extension was calculated as the length of the hole from the base of blade on

**Table 1.** Model parameters for each model fitted to thermal performance curves under both current and future $CO_2$. $T_{opt}$ = thermal optimum and $R_{max}$ = maximum rate at thermal optimum. Values are model estimates of each parameter with 95% confidence intervals in parentheses.

| response | $CO_2$ level | model | $T_{opt}$ | $R_{max}$ |
|---|---|---|---|---|
| growth (linear extension) | current | O'Neill *et al.* [44] | 16.05 (14.68–17. 30) | 1.01 (0.86–1.17) |
| | future | O'Neill *et al.* [44] | 15.72 (14.94–16.57) | 1.06 (0.94–1.27) |
| net photosynthesis | current | O'Neill *et al.* [44] | 16.67 (5.57–23.72) | 4.65 (3.72–5.82) |
| | future | O'Neill *et al.* [44] | 18.44 (16.30–21.34) | 7.48 (6.47–8.54) |
| change in weight % | current | Yan and Hunt [45] | 16.60 (15.39–18.06) | 43.04 (37.84–48.72) |
| | future | O'Neill *et al.* [44] | 14.80 (13.83–15.84) | 50.95 (38.14–64.96) |

day 21 minus length of hole from base of blade on day 1 and is expressed as mm $day^{-1}$. Wet weight was measured by weighing each individual after they were gently patted dry on day 1 and day 21. Change in wet weight was calculated as the percentage change from the initial weight on day 1.

### (ii) Net photosynthesis

Oxygen evolution in the light (net photosynthesis, a key indicator of performance) was measured on day 21 (i.e. after each individual had been exposed to experimental treatments for three weeks) for each of the five replicates per temperature and $CO_2$ combination. All incubations were conducted at the experimental irradiance and $CO_2$, and temperature was maintained at the appropriate levels for each treatment. Individuals were placed in sealed 260 ml glass chambers on an orbital shaker (OM7 Large Orbital Shaker, Ratek Instruments). Oxygen concentrations were measured at time = 0 and time = 3 h with a portable oxygen meter (Fibox 4, PreSens), coupled with a non-invasive oxygen sensor in each culture chamber (Oxygen Sensor Spot SP-PSt3-NAU, PreSens). Net photosynthesis is expressed as $\mu mol\, O_2\, g^{-1}\, h^{-1}$ wet weight. Values were corrected using the average change in oxygen concentration in three 'blank' control chambers containing no algae for each $CO_2$ and temperature combination.

### (iii) Stable C isotopes and C and N content

Stable isotope ratios were measured to provide evidence of inorganic carbon uptake strategies and C and N content were measured to provide indications on the nutrient status of the kelp. Samples for determination of $\delta^{13}C$ isotopic ratios and carbon and nitrogen content were destructively sampled and frozen at –20°C until all treatments had been measured. Following this, all samples were freeze dried (FreezeZone 4.5, Labconco) and kept at –20°C until later analysis. $\delta^{13}C$ isotopic ratios and carbon and nitrogen content were determined by weighing approximately 5 mg of dried tissue into tin cups (Sercon, UK) and analysed using an elemental analyser (NA1500, Fisons Instruments) coupled to an isotope ratio mass spectrometer (Delta V Plus, ThermoFisher Scientific) via a Universal Continuous Flow Interface (Conflo IV, ThermoFisher Scientific). Combustion and reduction were achieved at 1020°C and 650°C, respectively. Isotope values were normalized to the Vienna Pee Dee Belemnite scale via a three-point calibration using certified reference material and both precision and accuracy were ±0.1% (1 s.d.).

## (d) Statistical analysis

### (i) Model fitting and selection

All analyses were conducted in the statistical software program R v. 3.6.1 [53]. As multiple functions can be used to model TPCs, we fitted nine models that are commonly used for each response variable (growth, net photosynthesis and change in wet weight) at each $CO_2$ level. Briefly, each model followed a pattern typical of TPCs where performance increases from low temperatures until an optimum, after which performance rapidly declines. All models and their outputs and can be seen in electronic supplementary material, table S1 and further reading on each of the nine models can be found in Padfield *et al*. [54]—electronic supplementary material. The most appropriate model for each response and $CO_2$ level was chosen by firstly excluding all models that had a root mean square error (RMSE) greater than 2% of the best fitting model; secondly, we excluded models that were non-sensical (e.g. those that didn't follow a known pattern of thermal performance or included negative values where these were not possible such as linear extension), and thirdly if more than one model was deemed appropriate, the model with the most useful biological parameters was chosen with priority given to models that explicitly included thermal optima and maximum rate followed by critical thermal maximum. This approach was chosen as it balanced goodness of fit and useful biological information [55]. All models were fitted using nonlinear least squares using the package *rTPC* [56] or *stats* [53]. The parameters of each model were extracted from the best fit model using the *rTPC* package [54] with 95% confidence intervals around the model fits and parameter estimates derived by bootstrapping using the *car* package [57]. A quadratic function was used to model the effect of temperature on stable C isotopes for both current and future $CO_2$ levels. In the highest temperature treatment, mortality occurred in four individuals from the current $CO_2$ level and two from the future $CO_2$ level. Individuals were considered dead if they had both net photosynthetic rates of below zero and substantial loss of tissue. These individuals were excluded from the net photosynthesis models to avoid them having excessive influence on model fits. Tissue samples from the dead individuals were still included in measurements of stable C isotopes and C and N content, except for one in the current $CO_2$ level, which did not have enough remaining tissue for analyses due to tissue loss. A measurement error also resulted in the loss of one sample from the 20°C in each of the current and future $CO_2$ levels for net photosynthesis.

### (ii) Projections of thermal performance

To illustrate how thermal performance may change under different warming scenarios, we modelled annual thermal performance for growth, net photosynthesis and change in wet weight under three scenarios: (i) current: average daily SST between 2002 and 2020 at the collection site [43], (ii) future: average daily SST between 2002 and 2020 + 3°C, and (iii) future extreme: average daily SST between 2002 and 2020 + 4.5°. The two future scenarios were chosen to represent the upper end of projections of SST under RCP 4.5 and RCP 8.5 in 2090 for this region [58]. To model performance, we populated the models chosen to describe the experimental TPC responses for each response variable (i.e. those in table 1) for the SST conditions described above. Model fits under current $CO_2$ were used for the current scenario and model fits under elevated $CO_2$ were used for both future

scenarios. Model projections were made by using the *predFit* function in the *investr* package [59] with 95% confidence intervals calculated by bootstrapping in the *car* package [57]. All projections display change in performance relative to the current scenario and are expressed as percentage change in performance. As such, all projections display how thermal performance will vary relative to the present day and are not intended to be seen as projections of realized performance which will be influenced by a multitude of biotic and abiotic factors.

## 3. Results

### (a) Experimental culture conditions

Temperatures were maintained close to target values and ranged from a mean of 5.57°C in the lowest temperature treatment to 28.84°C in the highest temperature treatment. $pCO_2$ values were on average 421.98 ± 65.295 µatm (s.e.) in the current $CO_2$ treatments and 992.35 ± 151.90 (s.e.) in the future $CO_2$ treatments. There was some variation in $pCO_2$ levels within both current and future treatments ranging from 380 to 472 µatm in the current treatment and 840 to 1156 µatm in the future treatment, presumably due to the metabolic activity of the kelp altering inorganic carbon concentrations. Electronic supplementary material, table S2 shows the specific means and standard errors for temperature and $pCO_2$ for each of the 16 treatment combinations. Nitrate and ammonium concentrations measured just prior to a water change were 1.28 µM ± 0.22 and 0.54 µM ± 0.42 respectively (means and s.d., $n = 47$).

### (b) Biotic responses

#### (i) Growth (linear extension), net photosynthesis and change in wet weight (%)

Linear extension, net photosynthesis and change in wet weight all followed patterns typical of TPCs with rates increasing from low temperatures until an optimum, followed by a decline at temperatures beyond the optimum (figure 1). There was minimal effect of $CO_2$ on linear extension rates with near identical curves fitting both data and thermal optimum and maximum growth rates being similar, with overlapping confidence intervals (table 1). For net photosynthesis, thermal optima were similar under both current and future $CO_2$ levels with similar means (current = 16.86, future = 18.01) and overlapping confidence intervals (current = 5.57–20.43, future = 16.50–19.56, table 1). However, the maximum rate of net photosynthesis at these optima differed (mean current = 4.67 µmol $O_2$ $l^{-1}$ $g^{-1}$ $h^{-1}$, mean future = 7.28 µmol $O_2$ $l^{-1}$ $g^{-1}$ $h^{-1}$) and 95% confidence intervals did not overlap (current = 3.80–5.85 µmol $O_2$ $l^{-1}$ $g^{-1}$ $h^{-1}$, future = 6.49–8.56 µmol $O_2$ $l^{-1}$ $g^{-1}$ $h^{-1}$, table 1). Changes in wet weight were similar between current and future $CO_2$ levels for both thermal optima and maximum rate of change (overlapping confidence intervals, table 1). However, there was substantially greater tissue loss at 28.84°C in the current $CO_2$ level treatment as evidenced by percentage change in weight (means ± 95% confidence intervals: current = −63.06 ± 49.68, future = −4.71 ± 13.63).

#### (ii) Stable C isotopes and C : N ratios

Carbon stable isotope values followed a pattern of being reduced at low temperatures, increasing until approximately 16°C and then declining until the highest temperature (electronic supplementary material, figure S1). This pattern was well described by a quadratic function for both $CO_2$ scenarios, and model fits were similar for both current and future $CO_2$ levels with overlapping confidence intervals. Means ± s.e. for % N, % C and C : N at each temperature and $CO_2$ level are shown in table 2.

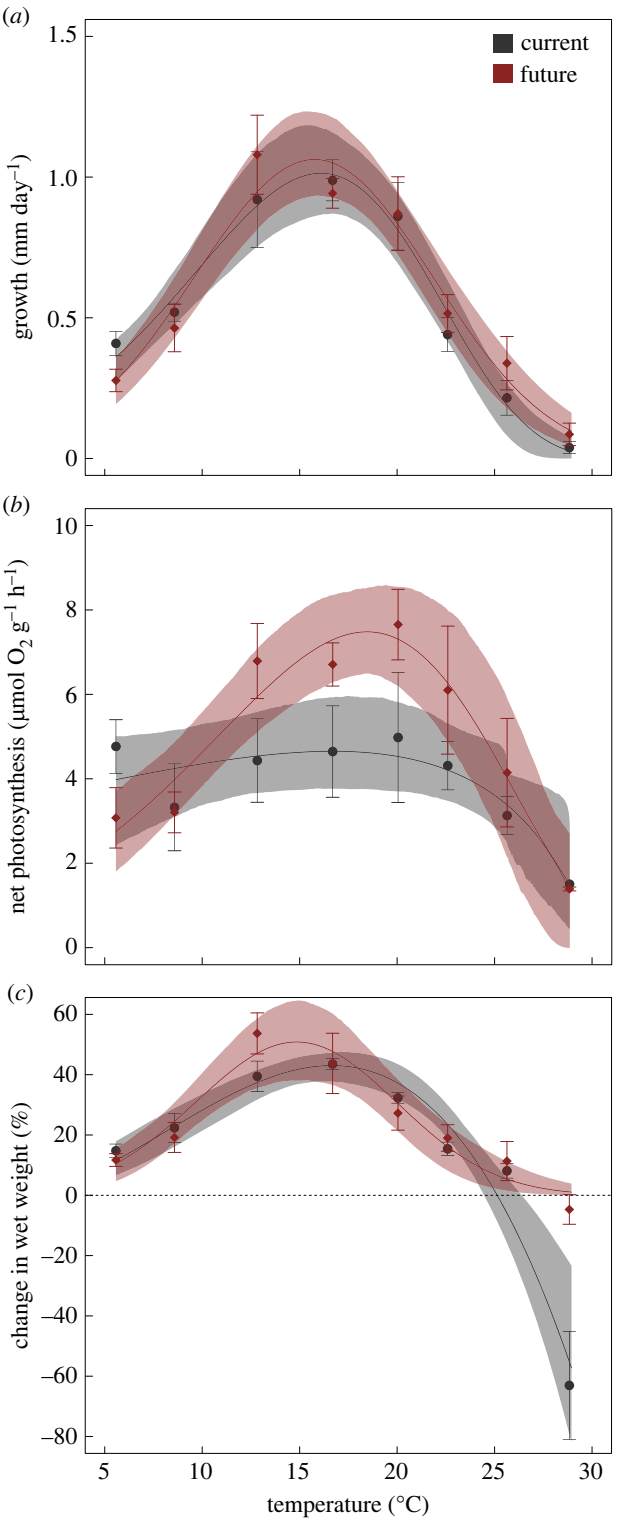


**Figure 1.** Thermal response curves of *E. radiata* individuals cultured at 5.87–28.84°C under current (422 µatm, grey lines) and future (992 µatm, red lines) $pCO_2$ conditions. Shaded areas refer to 95% confidence intervals of model fits. Grey circles refer to mean values under current $pCO_2$ and red diamonds refer to mean values under future $pCO_2$, error bars are standard error, $n = 1$–5 for each temperature and $pCO_2$ combination. (*a*) growth (mm $d^{-1}$), (*b*) net photosynthesis (µmol $O_2$ $l^{-1}$ $g^{-1}$ $h^{-1}$), (*c*) change in wet weight (%).

**Table 2.** Means and standard error for % C, % N and C : N ratios in *E. radiata* cultured at each temperature under both current and future $pCO_2$ levels.

| $CO_2$ level | Temperature °C | % C | s.e. | % N | s.e. | C : N | s.e. |
|---|---|---|---|---|---|---|---|
| **current** | 5.57 | 33.3 | 0.45 | 1.1 | 0.03 | 30.5 | 1.0 |
| | 8.58 | 35.9 | 1.07 | 1.3 | 0.18 | 29.5 | 3.1 |
| | 12.82 | 33.3 | 0.54 | 1.0 | 0.07 | 31.8 | 2.0 |
| | 16.69 | 35.1 | 0.45 | 0.9 | 0.02 | 36.6 | 0.7 |
| | 20.04 | 32.2 | 0.64 | 0.9 | 0.02 | 32.7 | 0.9 |
| | 22.59 | 28.9 | 0.61 | 0.9 | 0.02 | 29.7 | 1.0 |
| | 25.63 | 34.2 | 0.57 | 1.0 | 0.04 | 32.2 | 1.0 |
| | 28.84 | 28.7 | 0.76 | 1.4 | 0.11 | 20.8 | 2.5 |
| **future** | 5.57 | 34.4 | 0.56 | 1.1 | 0.04 | 29.5 | 1.3 |
| | 8.58 | 36.5 | 0.32 | 1.0 | 0.02 | 36.2 | 1.0 |
| | 12.82 | 33.5 | 0.30 | 1.0 | 0.02 | 33.7 | 0.7 |
| | 16.69 | 34.3 | 0.42 | 1.0 | 0.02 | 36.2 | 0.4 |
| | 20.04 | 33.0 | 0.36 | 1.0 | 0.04 | 34.9 | 1.4 |
| | 22.59 | 29.9 | 0.50 | 0.9 | 0.04 | 31.3 | 1.1 |
| | 25.63 | 35.1 | 0.76 | 1.0 | 0.03 | 34.5 | 1.7 |
| | 28.84 | 27.6 | 0.99 | 1.4 | 0.10 | 19.7 | 1.9 |

### (c) Projections

Modelled annual thermal performance varied considerably in both warming scenarios (figure 2). All percentage changes are relative to thermal performance under present thermal regimes using the elevated $CO_2$ models. When imposing an additional 3°C on baseline temperatures to simulate future ocean conditions the model indicated an increase in growth rates during late winter and early spring (August–October, peak 26% increase) and a decrease during late summer and early autumn (February–April, peak 17% decrease). A similar pattern was observed for change in weight, with a peak increase of 46% in spring and a peak decrease of 29% early autumn. By contrast, net photosynthetic rates increased at all stages of the year (51–61% increase). Imposing a 4.5°C increase on current baseline temperatures to simulate an extreme warming scenario indicated that in winter and early spring growth rates would increase (peak 26%) and decrease in late summer and early autumn (peak 33%). Photosynthetic rates increased throughout the year (47–63% increase), while weight change increased in winter and spring (peak 39% increase) and decreased by in late summer and autumn (peak 49% decrease).

## 4. Discussion

We measured thermal performance of juveniles of the habitat forming kelp *E. radiata* from a population at the cool edge of its distribution under ambient and elevated $CO_2$, to identify thermal optima and tolerance and whether these were influenced by elevated $CO_2$. Optimum temperatures for growth and photosynthesis were unaffected by $CO_2$ and were substantially lower (approx. 6°C) than reported for sporophytes of *E. radiata* at the warm edge of its distribution [15]. Maximum growth rates were unaffected by $CO_2$; however, maximum net photosynthetic rates were 59% higher under elevated $CO_2$. Using modelled thermal performance under both current and future $CO_2$ conditions and historical SST data, we projected performance under future global ocean change scenarios. These model projections identified that this cool-edge population of *E. radiata* in Australia is susceptible to ocean warming and marine heatwaves in late summer and early autumn. This highlights the importance of understanding and mitigating additional stressors over these periods of risk and has implications for reproductive phenology, productivity, and more broadly for the seasonality of restoration and aquaculture.

### (a) $CO_2$: effect on growth and photosynthesis across temperatures

Elevated $CO_2$ had varying effects on the performance of *E. radiata* juveniles across temperatures. Growth rates were unaffected, except for tissue loss being mitigated under elevated $CO_2$ at temperatures above 26°C. The lack of an increase in thermal tolerance was unexpected as elevated $CO_2$ has been shown to increase thermal performance in the fucoid *P. comosa* [34], as have elevated concentrations of inorganic nitrogen in the kelp *M. pyrifera* [35]. In contrast to growth, rates of net photosynthesis increased, but only around the optimum temperatures (i.e. changes in the *Y*-axis of the TPC). The decoupling of the growth and photosynthetic response is not surprising as increases in photosynthetic rate due to elevated $CO_2$ are not always paralleled by differences in growth rate [60]. However, the mechanisms driving the elevated photosynthetic rates around thermal optimum are unclear. Carbon isotope discrimination values suggested the presence of a CCM in *E. radiata* [32,61], yet we found no evidence for the downregulation of the CCMs as previously observed in *E. radiata* [62]. It is possible that elevated $CO_2$ stimulated an increase in Rubisco content as seen in green

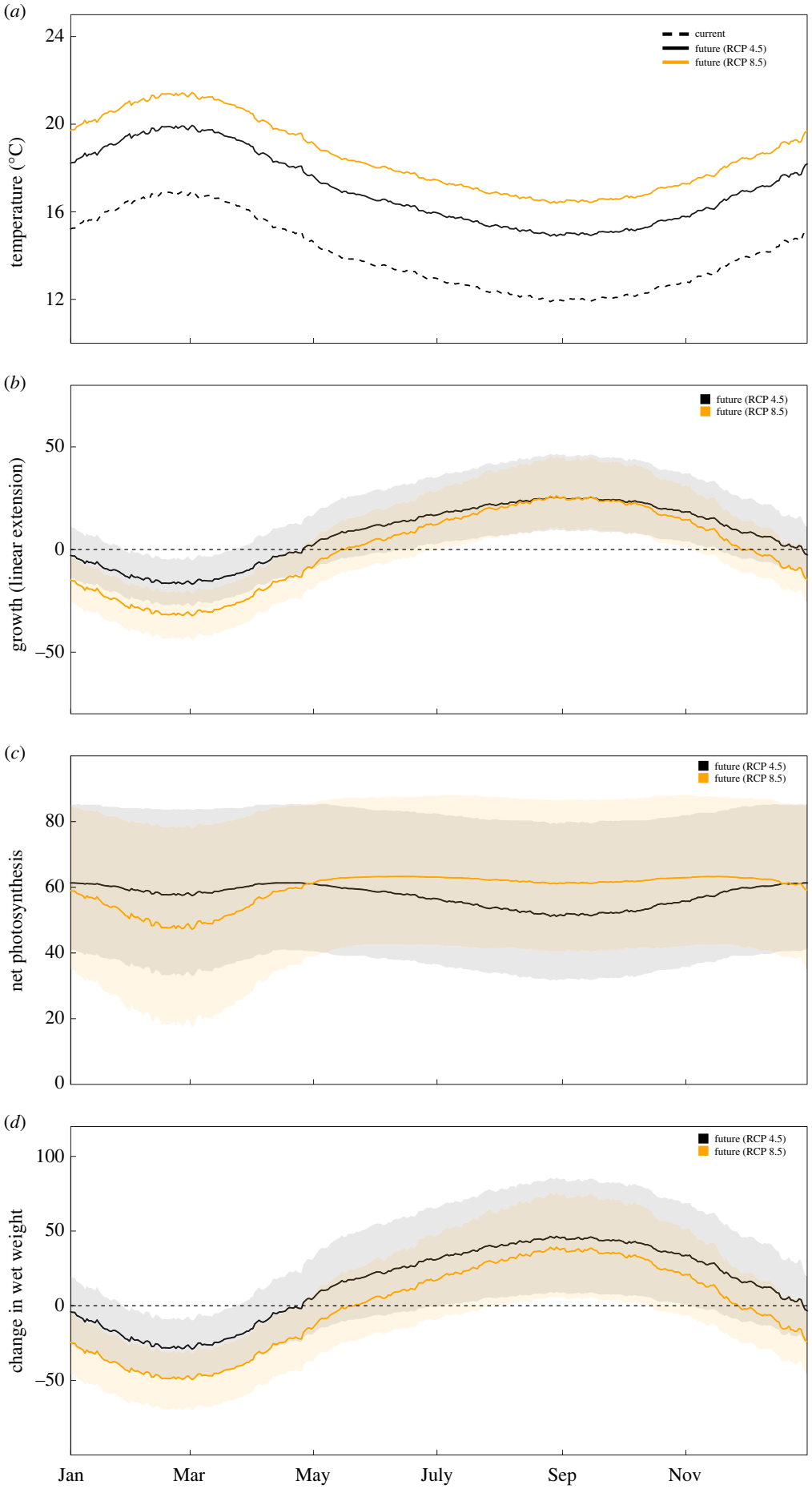


**Figure 2.** Modelled annual performance of *E. radiata* over the course of a year based on average SST at the collection site and additional increases in temperature to simulate global ocean change scenarios (note that this is a Southern Hemisphere site, thus January is summer). Performance is displayed as % increase or decrease relative to current conditions. (*a*) daily SST average in each scenario at collection site, (*b*) growth (linear extension), (*c*) net photosynthesis, (*d*) change in wet weight. Shaded areas refer to 95% confidence intervals of model fits.

algae [63]. However, stress associated with extreme temperatures was probably limiting photosynthetic rates at the extremes [64], meaning *E. radiata* was unable to benefit from the additional $CO_2$. Alternatively, the specificity factor of Rubisco for $CO_2/O_2$ generally decreases with elevated temperatures [65], which could have limited net photosynthesis above the optima due to increases in photorespiration. While at lower temperatures, rates of chemical reactions are limited by temperature and additional Rubisco would need to be synthesized to increase photosynthetic rates [66]. However, since we did not measure Rubisco kinetics or content, we are unable to identify specific mechanisms. Further research using molecular tools such as transcriptomics and gene expression would assist in elucidating some of these putative mechanisms.

### (b) Warming profiles and local adaptation

The thermal optimum for this cool-edge *E. radiata* population was substantially (6–8°C) lower than reported previously for the species from the warm edge of its distribution ([15], approx. 24°C). It is important to note that the study of Wernberg *et al*. [15] measured short-term (45 min) incubations, whereas our study was conducted over three weeks, making direct comparisons difficult. Nevertheless, this observed difference in thermal optima may indicate substantial acclimatization or adaptation of *E. radiata* populations to local temperature conditions [67,68], supporting previous findings of similar adaptation or acclimatization for the gametophyte life stage [41,69]. Moreover, the difference in optima is similar to the difference in annual mean SST between our site and those in Wernberg *et al*. [15] of approximately 6–8°C, further suggesting acclimatization or adaptation to local temperatures. This has implications for the cool-edge populations of *E. radiata* as they may be more susceptible to warming and marine heatwaves than was previously thought (e.g. [14]).

While it is unclear whether the differences we observed are due to acclimatization, adaptation or some combination of both, understanding these mechanisms is critical to assessing overall susceptibility to warming. If their thermal tolerance is related to a distinct genetic identity and adapted cluster of cool-edge populations, there may be limited capacity to respond and overcome the projected increases in ocean warming [68,70,71]. Alternatively, since thermal performance can be a plastic trait that responds to environmental conditions (particularly at juvenile life-history stages, [72,73]), cool-edge populations may be able to respond and acclimatize as the region continues to warm. Critically, however, both the magnitude of warming and genetic connectivity are likely to be key determinants of future adaptive responses along thermal gradients [68,74]. Connectivity between *E. radiata* populations varies across its range but can be reasonably high [75]; although whether it is sufficient to facilitate adaptation in this global ocean warming hotspot [38] remains to be tested. Reciprocal transplants or common garden experiments could help characterize and differentiate patterns of adaptive potential, while further population genetic work is also needed to better understand broader patterns of gene flow across the species' range.

### (c) Identifying susceptible periods, and implications

The modelled annual profiles of *E. radiata* performance suggest juveniles of *E. radiata* at this location are most susceptible to global ocean change in late summer and early autumn, with growth rates declining in all modelled warming scenarios. However, these scenarios did not consider the influence of other key seasonal drivers of kelp performance such as light intensity, daylength, nutrient concentrations and grazing rates (e.g. [76,77]), and thus should not be considered a measure of realized performance over the course of a year. Regardless, they are valuable in providing indications of during which time periods *E. radiata* is likely to be under thermal stress. Identifying these time periods is critically important given the highly seasonal demographic patterns of *E. radiata* and kelps in general [76,78]. For example, highest thermal stress occurs in late summer and early autumn, which are the peak periods of growth for adult and juvenile *E. radiata* [79,80] and coincide with peak spore production for *E. radiata* in Tasmania [76,81]. Thus, increased thermal stress during that period may have particularly significant impacts on *E. radiata* population dynamics and subtidal kelp communities, beyond reductions in the growth rates of individuals.

The modelled projections of performance also highlighted likely periods of elevated growth in spring because of temperatures becoming closer to optimum during this time. This has implications for the timing of restoration interventions or aquaculture operations [80,82,83], and for broader ecosystem productivity during spring blooms. Yet, it is unlikely that these forecast periods of elevated growth would offset the negative impacts that arise during the period of increased thermal stress, particularly if marine heatwave events, which are predicted to increase in intensity and frequency, impose further thermal stress [84,85]. For example, if a thermal stress is severe enough in late summer/early autumn, there may be few *E. radiata* remaining to benefit from improved springtime growth rates. Even in less extreme cases, pervasive sublethal effects during periods of high stress may shape broader population dynamics into a sort of annual crash-and-recovery pattern (e.g. [86]). Similar patterns seem increasingly evident in giant kelp (*M. pyrifera*) in Tasmania (C Layton 2023, personal observation, [10]), which has experienced dramatic declines despite local seawater temperatures being within a suitable range for the species throughout much of the year, although this is probably in part also driven by nutrient limitation [10,17]. The loss, or reduced performance, of canopy-forming adults of *E. radiata* during periods of increased stress may also impact the growth and survivorship of juvenile conspecifics and the overall resilience and recovery potential of the system [80]. Analysing whether and how population dynamics of *E. radiata* will be impacted by warming and marine heatwaves in the natural setting should be a priority of future research. Characterizing patterns of intraspecific variability at regional and individual levels should also help to identify populations that may be particularly susceptible or resilient to ocean change (e.g. [17,74]), even for cool-edge populations that may be at higher risk of thermal stress than previously thought.

## 5. Conclusion

Typically, warm-edge populations of organisms, living near their thermal maximum, are considered more threatened by warming and local extinctions and range contractions. By contrast, cool-edge populations may be expected to benefit as

warming increases temperatures towards the thermal optima for the species. However, here we show that thermal optima for sporophytes from a cool-edge population of the habitat forming kelp *E. radiata* can be substantially lower than that of warm-edge conspecifics, probably due to acclimatization/adaptation to local temperature regimes. Furthermore, we show that their thermal tolerance and optima are unlikely to be enhanced under the forecast increases in $CO_2$ that are occurring alongside warming. Indeed, projections of global ocean change scenarios indicate that this cool-edge population of *E. radiata* is likely to become increasingly impacted in a future ocean. Given the geographical isolation of cool-edge populations of *E. radiata* in Tasmania and the lack of a benefit of elevated $CO_2$, these cool-edge populations may be more threatened by warming than previously recognized. It is likely that rapid acclimatization/adaptation of *E. radiata* populations at regional scales may be required to counteract the negative effects of warming and marine heatwave events.

Ethics. This work did not require ethical approval from a human subject or animal welfare committee.

Data accessibility. The data are provided in electronic supplementary material [87].

Declaration of AI use. We have not used AI-assisted technologies in creating this article.

Authors' contributions. D.B.: conceptualization, data curation, formal analysis, investigation, methodology, writing—original draft, writing—review and editing; C.L.: conceptualization, data curation, formal analysis, investigation, methodology, writing—original draft, writing—review and editing; C.N.M.: formal analysis, writing—review and editing; E.A.B.: formal analysis, methodology, writing—review and editing; J.D.G.-E.: conceptualization, formal analysis, funding acquisition, writing—review and editing; J.B.: formal analysis, funding acquisition, writing—review and editing; J.A.R.: formal analysis, funding acquisition, writing—review and editing; C.L.H.: conceptualization, formal analysis, funding acquisition, supervision, writing—review and editing.

All authors gave final approval for publication and agreed to be held accountable for the work performed therein.

Competing interests. The authors declare that there are no competing interests.

Funding. The research was funded by an Australian Research Council Discovery Project to C.L.H., J.B., J.D.G.-E. and J.A.R. (grant no: DP200101467).

Acknowledgements. We would like to thank Allyson Nardelli, Olivia Wynn, Eva Smid, Pam Quayle and Axel Durand for assistance in the laboratory and the field. We would also like to thank Mridul Thomas for expert advice on the analysis of thermal performance data.

## References

1. Intergovernmental Panel on Climate Change (IPCC). 2023 *Climate change 2021: the physical science basis. Contribution of working group I to the sixth assessment report of the Intergovernmental Panel on Climate Change*. Cambridge, UK: Cambridge University Press. (doi:10.1017/9781009157896)
2. Poloczanska ES *et al.* 2016 Responses of marine organisms to climate change across oceans. *Front. Mar. Sci.* **3**, 62. (doi:10.3389/fmars.2016.00062)
3. Smale DA. 2020 Impacts of ocean warming on kelp forest ecosystems. *New Phytol.* **225**, 1447–1454. (doi:10.1111/nph.16107)
4. Steneck RS, Graham MH, Bourque BJ, Corbett D, Erlandson JM, Estes JA, Tegner MJ. 2002 Kelp forest ecosystems: biodiversity, stability, resilience and future. *Environ. Conserv.* **29**, 436–459. (doi:10.1017/S0376892902000322)
5. Steneck R, Johnson C. 2013 Kelp forests: dynamic patterns, processes, and feedbacks. In *Marine community ecology and conservation* (eds M Bertness, J Bruno, B Silliman, J Stachowicz), pp. 315–336. Sunderland, MA: Sinauer Associates, Inc.
6. Krumhansl KA *et al.* 2016 Global patterns of kelp forest change over the past half-century. *Proc. Natl Acad. Sci. USA* **113**, 13 785–13 790. (doi:10.1073/pnas.1606102113)
7. Vergés A, McCosker E, Mayer-Pinto M, Coleman MA, Wernberg T, Ainsworth T, Steinberg PD. 2019 Tropicalisation of temperate reefs: implications for ecosystem functions and management actions. *Funct. Ecol.* **33**, 1000–1013. (doi:10.1111/1365-2435.13310)
8. Boyd PW *et al.* 2018 Experimental strategies to assess the biological ramifications of multiple drivers of global ocean change—a review. *Glob. Change Biol.* **24**, 2239–2261. (doi:10.1111/gcb.14102)
9. Hurd CL, Lenton A, Tilbrook B, Boyd PW. 2018 Current understanding and challenges for oceans in a higher-$CO_2$ world. *Nat. Clim. Change* **8**, 686–694. (doi:10.1038/s41558-018-0211-0)
10. Butler CL, Lucieer VL, Wotherspoon SJ, Johnson CR. 2020 Multi-decadal decline in cover of giant kelp *Macrocystis pyrifera* at the southern limit of its Australian range. *Mar. Ecol. Progress Series* **653**, 1–18. (doi:10.3354/meps13510)
11. Hobday AJ *et al.* 2016 A hierarchical approach to defining marine heatwaves. *Prog. Oceanogr.* **141**, 227–238. (doi:10.1016/j.pocean.2015.12.014)
12. Wernberg T *et al.* 2016 Climate-driven regime shift of a temperate marine ecosystem. *Science* **353**, 169–172. (doi:10.1126/science.aad8745)
13. Thomsen MS, Mondardini L, Alestra T, Gerrity S, Tait L, South PM, Lilley SA, Schiel DR. 2019 Local extinction of bull kelp (*Durvillaea* spp.) due to a marine heatwave. *Front. Mar. Sci.* **6**, 84. (doi:10.3389/fmars.2019.00084)
14. Martínez B *et al.* 2018 Distribution models predict large contractions of habitat-forming seaweeds in response to ocean warming. *Divers. Distrib.* **24**, 1350–1366. (doi:10.1111/ddi.12767)
15. Wernberg T, de Bettignies T, Joy BA, Finnegan PM. 2016 Physiological responses of habitat-forming seaweeds to increasing temperatures. *Limnol. Oceanogr.* **61**, 2180–2190. (doi:10.1002/lno.10362)
16. Bennett S, Vaquer-Sunyer R, Jordá G, Forteza M, Roca G, Marbà N. 2022 Thermal performance of seaweeds and seagrasses across a regional climate gradient. *Front. Mar. Sci.* **9**, 733315. (doi:10.3389/fmars.2022.733315)
17. Layton C, Johnson CR. 2021 *Assessing the feasibility of restoring giant kelp forests in Tasmania*. Report to the National Environmental Science Program, Marine Biodiversity Hub. Battery Point, Australia: Institute for Marine and Antarctic Studies, University of Tasmania.
18. King NG, McKeown NJ, Smale DA, Wilcockson DC, Hoelters L, Groves EA, Stamp T, Moore PJ. 2019 Evidence for different thermal ecotypes in range centre and trailing edge kelp populations. *J. Exp. Mar. Biol. Ecol.* **514–515**, 10–17. (doi:10.1016/j.jembe.2019.03.004)
19. Bennett S, Wernberg T, Joy BA, De Bettignies T, Campbell AH. 2015 Central and rear-edge populations can be equally vulnerable to warming. *Nat. Commun.* **6**, 10280. (doi:10.1038/ncomms10280)
20. Howells EJ, Berkelmans R, van Oppen MJH, Willis BL, Bay LK. 2013 Historical thermal regimes define limits to coral acclimatization. *Ecology* **94**, 1078–1088. (doi:10.1890/12-1257.1)
21. Jury CP, Toonen RJ. 2019 Adaptive responses and local stressor mitigation drive coral resilience in warmer, more acidic oceans. *Proc. Biol. Sci.* **286**, 1–9.
22. Sandoval-Castillo J, Robinson NA, Hart AM, Strain LWS, Beheregaray LB. 2018 Seascape genomics reveals adaptive divergence in a connected and commercially important mollusc, the greenlip abalone (*Haliotis laevigata*), along a longitudinal environmental gradient. *Mol. Ecol.* **27**, 1603–1620. (doi:10.1111/mec.14526)

23. Sanford E, Kelly MW. 2010 Local adaptation in marine invertebrates. *Annu. Rev. Mar. Sci.* **3**, 509–535. (doi:10.1146/annurev-marine-120709-142756)
24. Angilletta MJ. 2006 Estimating and comparing thermal performance curves. *J. Therm. Biol* **31**, 541–545. (doi:10.1016/j.jtherbio.2006.06.002)
25. Sinclair BJ *et al.* 2016 Can we predict ectotherm responses to climate change using thermal performance curves and body temperatures? *Ecol. Lett.* **19**, 1372–1385. (doi:10.1111/ele.12686)
26. Connell SD, Russell BD. 2010 The direct effects of increasing $CO_2$ and temperature on non-calcifying organisms: increasing the potential for phase shifts in kelp forests. *Proc. R. Soc. B* **277**, 1409–1415. (doi:10.1098/rspb.2009.2069)
27. Zayas-Santiago CC, Rivas-Ubach A, Kuo LJ, Ward ND, Zimmerman RC. 2020 Metabolic profiling reveals biochemical pathways responsible for eelgrass response to elevated $CO_2$ and temperature. *Sci. Rep.* **10**, 4693. (doi:10.1038/s41598-020-61684-x)
28. Harrington AM, Harrington RJ, Bouchard DA, Hamlin HJ. 2020 The synergistic effects of elevated temperature and $CO_2$-induced ocean acidification reduce cardiac performance and increase disease susceptibility in subadult, female American lobsters *Homarus americanus* H. Milne Edwards, 1837 (Decapoda: Astacidea: Nephropidae) from the Gulf of Maine. *J. Crustacean Biol.* **40**, 634–646. (doi:10.1093/jcbiol/ruaa041)
29. Connell SD, Kroeker KJ, Fabricius KE, Kline DI, Russell BD. 2013 The other ocean acidification problem: $CO_2$ as a resource among competitors for ecosystem dominance. *Phil. Trans. R. Soc. B* **368**, 20120442. (doi:10.1098/rstb.2012.0442)
30. Kroeker KJ, Kordas RL, Crim R, Hendriks IE, Ramajo L, Singh GS, Duarte CM, Gattuso JP. 2013 Impacts of ocean acidification on marine organisms: quantifying sensitivities and interaction with warming. *Glob. Change Biol.* **19**, 1884–1896. (doi:10.1111/gcb.12179)
31. Giordano M, Beardall J, Raven JA. 2005 $CO_2$ concentrating mechanisms in algae: mechanisms, environmental modulation, and evolution. *Annu. Rev. Plant Biol.* **56**, 99–131. (doi:10.1146/annurev.arplant.56.032604.144052)
32. Raven JA, Ball LA, Beardall J, Giordano M, Maberly SC. 2005 Algae lacking carbon-concentrating mechanisms. *Canad. J. Bot.* **83**, 879–890. (doi:10.1139/b05-074)
33. Raven JA. 2011 Effects on marine algae of changed seawater chemistry with increasing atmospheric $CO_2$. *Biol. Environ.* **111**, 1–17. (doi:10.3318/BIOE.2011.01)
34. Britton D *et al.* 2020 Adjustments in fatty acid composition is a mechanism that can explain resilience to marine heatwaves and future ocean conditions in the habitat-forming seaweed *Phyllospora comosa* (Labillardière) C.Agardh. *Glob. Change Biol.* **26**, 3512–3524. (doi:10.1111/gcb.15052)
35. Fernández PA, Gaitán-Espitia JD, Leal PP, Schmid M, Revill AT, Hurd CL. 2020 Nitrogen sufficiency enhances thermal tolerance in habitat-forming kelp: implications for acclimation under thermal stress. *Sci. Rep.* **10**, 3186. (doi:10.1038/s41598-020-60104-4)
36. Schmid M, Fernández PA, Gaitán-Espitia JD, Virtue P, Leal PP, Revill AT, Nichols PD, Hurd CL. 2020 Stress due to low nitrate availability reduces the biochemical acclimation potential of the giant kelp *Macrocystis pyrifera* to high temperature. *Algal Res.* **47**, 101895. (doi:10.1016/j.algal.2020.101895)
37. AbdElgawad H, Farfan-Vignolo ER, Vos DD, Asard H. 2015 Elevated $CO_2$ mitigates drought and temperature-induced oxidative stress differently in grasses and legumes. *Plant Sci.* **231**, 1–10. (doi:10.1016/j.plantsci.2014.11.001)
38. Hobday AJ, Pecl GT. 2014 Identification of global marine hotspots: sentinels for change and vanguards for adaptation action. *Rev. Fish Biol. Fish.* **24**, 415–425. (doi:10.1007/s11160-013-9326-6)
39. Johnson CR *et al.* 2011 Climate change cascades: shifts in oceanography, species' ranges and subtidal marine community dynamics in eastern Tasmania. *J. Exp. Mar. Biol. Ecol.* **400**, 17–32. (doi:10.1016/j.jembe.2011.02.032)
40. Wernberg T *et al.* 2019 Biology and ecology of the globally significant kelp *Ecklonia radiata*. *Oceanogr. Mar. Biol. Annu. Rev.* **57**, 265–323. (doi:10.1201/9780429026379-6)
41. Mohring M, Wernberg T, Wright J, Connell S, Russell B. 2014 Biogeographic variation in temperature drives performance of kelp gametophytes during warming. *Mar. Ecol. Progress Series* **513**, 85–96. (doi:10.3354/meps10916)
42. Young MA, Critchell K, Miller AD, Treml EA, Sams M, Carvalho R, Ierodiaconou D. 2023 Mapping the impacts of multiple stressors on the decline in kelps along the coast of Victoria, Australia. *Divers. Distrib.* **29**, 199–220. (doi:10.1111/ddi.13654)
43. Banzon V, Smith TM, Chin TM, Liu C, Hankins W. 2016 A long-term record of blended satellite and in situ sea-surface temperature for climate monitoring, modeling and environmental studies. *Earth System Sci. Data* **8**, 165–176. (doi:10.5194/essd-8-165-2016)
44. O'Neill RV, Goldstein RA, Shugart HH, Mankin JB. 1972 *Terrestrial ecosystem energy model: Eastern Deciduous Forest Biome memo report*. Oak Ridge, TN: The Environmental Sciences Division of the Oak Ridge National Laboratory.
45. Yan W, Hunt LA. 1999 An equation for modelling the temperature response of plants using only the cardinal temperatures. *Ann. Bot.* **84**, 607–614. (doi:10.1006/anbo.1999.0955)
46. McGraw CM, Cornwall CE, Reid MR, Currie KI, Hepburn CD, Boyd P, Hurd CL, Hunter KA. 2010 An automated pH-controlled culture system for laboratory-based ocean acidification experiments. *Limnol. Oceanogr. Methods* **8**, 686–694.
47. Dickson AG, Sabine CL, Christian JR. 2007 *Guide to best practices for ocean $CO_2$ measurements*. Sidney, Canada: North Pacific Marine Science Organization. (doi:10.25607/OBP-1342)
48. Lewis E, Wallace DWR. 1998 *Program developed for $CO_2$ systems calculations*. Oak Ridge, TN: ORNL/CDIAC-105 Carbon Dioxide Information Analysis Centre, Oak Ridge National Laboratory, US Department of Energy.
49. Mehrbach C, Culberson CH, Hawley JE, Pytkowicx RM. 1973 Measurement of the apparent dissociation constants of carbonic acid in seawater at atmospheric pressure. *Limnol. Oceanogr.* **18**, 897–907. (doi:10.4319/lo.1973.18.6.0897)
50. Lueker TJ, Dickson AG, Keeling CD. 2000 Ocean $pCO_2$ calculated from dissolved inorganic carbon, alkalinity, and equations for $K_1$ and $K_2$: validation based on laboratory measurements of $CO_2$ in gas and seawater at equilibrium. *Mar. Chem.* **70**, 105–119. (doi:10.1016/S0304-4203(00)00022-0)
51. Mann EH, Kirkman H. 1981 Biomass method for measuring productivity of *Ecklonia radiata*, with the potential for adaptation to other large brown algae. *Aus. J. Mar. Freshw. Res.* **32**, 297–304.
52. Schindelin J *et al.* 2012 Fiji: an open-source platform for biological-image analysis. *Nat. Methods* **9**, 676–682. (doi:10.1038/nmeth.2019)
53. R Core Team. 2019 *R: a language and environment for statistical computing*. Vienna, Austria: R Foundation for Statistical Computing. See https://www.R-project.org/.
54. Padfield D, O'Sullivan H, Pawar S. 2021 rTPC and nls.multstart: a new pipeline to fit thermal performance curves in R. *Methods Ecol. Evol.* **12**, 1138–1143. (doi:10.1111/2041-210X.13585)
55. Adams MP, Collier CJ, Uthicke S, Ow YX, Langlois L, O'Brien KR. 2017 Model fit versus biological relevance: evaluating photosynthesis-temperature models for three tropical seagrass species. *Sci. Rep.* **7**, 39930. (doi:10.1038/srep39930)
56. Padfield D, O'Sullivan H. 2021 *rTPC: functions for fitting thermal performance curves. R package version 1.0.2*. See https://cran.r-project.org/web/packages/rTPC/rTPC.pdf.
57. Fox J, Weisberg S. 2019 *An {R} companion to applied regression*, 3rd edn. Thousand Oaks, CA: Sage. https://socialsciences.mcmaster.ca/jfox/Books/Companion/.
58. CSIRO and Bureau of Meteorology. 2015 *Climate change in Australia*, Technical Report. Melbourne, Australia. See https://www.climatechangeinaustralia.gov.au.
59. Greenwell BM, Schubert Kabban CM. 2014 investr: an R Package for Inverse Estimation. *R J.* **6**, 90–100. (doi:10.32614/RJ-2014-009)
60. van der Loos LM, Schmid M, Leal PP, McGraw CM, Britton D, Revill AT, Virtue P, Nichols PD, Hurd CL. 2019 Responses of macroalgae to $CO_2$ enrichment cannot be inferred solely from their inorganic carbon uptake strategy. *Ecol. Evol.* **9**, 125–140. (doi:10.1002/ece3.4679)
61. Stepien CC. 2015 Impacts of geography, taxonomy and functional group on inorganic carbon use patterns in marine macrophytes. *J. Ecol.* **103**, 1372–1383. (doi:10.1111/1365-2745.12451)
62. Britton D, Cornwall CE, Revill AT, Hurd CL, Johnson CR. 2016 Ocean acidification reverses the positive effects of seawater pH fluctuations on growth and photosynthesis of the habitat-forming kelp, *Ecklonia radiata*. *Sci. Rep.* **6**, 26036. (doi:10.1038/srep26036)

63. Yokota A, David TC. 1985 Ribulose bisphosphate carboxylase/oxygenase content determined with $^{14}C$ carboxypentitol bisphosphate in plants and algae. *Plant Physiol.* **77**, 735–739. (doi:10.1104/pp.77.3.735)
64. Eggert A. 2012 Seaweed responses to temperature. In *Seaweed biology: novel insights into ecophysiology, ecology and utilization* (eds C Wiencke, K Bischof), pp. 47–66. Berlin, Germany: Springer.
65. Galmés J, Hermida-Carrera C, Laanisto L, Niinemets Ü. 2016 A compendium of temperature responses of Rubisco kinetic traits: variability among and within photosynthetic groups and impacts on photosynthesis modeling. *J. Exp. Bot.* **67**, 5067–5091. (doi:10.1093/jxb/erw267)
66. Young JN, Goldman JAL, Kranz SA, Tortell PD, Morel FMM. 2015 Slow carboxylation of Rubisco constrains the rate of carbon fixation during Antarctic phytoplankton blooms. *New Phytol.* **205**, 172–181. (doi:10.1111/nph.13021)
67. Alsuwaiyan NA, Vranken S, Filbee-Dexter K, Cambridge M, Coleman MA, Wernberg T. 2021 Genotypic variation in response to extreme events may facilitate kelp adaptation under future climates. *Mar. Ecol. Progress Series* **672**, 111–121. (doi:10.3354/meps13802)
68. Vranken S, Wernberg T, Scheben A, Severn-Ellis AA, Batley J, Bayer PE, Edwards D, Wheeler D, Coleman MA. 2021 Genotype–environment mismatch of kelp forests under climate change. *Mol. Ecol.* **30**, 3730–3746. (doi:10.1111/mec.15993)
69. Veenhof RJ, Champion C, Dworjanyn SA, Wernberg T, Minne AJP, Layton C, Bolton JJ, Reed DC, Coleman MA. 2022 Kelp gametophytes in changing oceans. In *Oceanography and marine biology: an annual review*, Vol. 60 (eds SJ Hawkins *et al.*), pp. 335–371. Boca Raton, FL: CRC Press.
70. Pearson GA, Logo-Leston A, Mota C. 2009 Frayed at the edges: selective pressure and adaptive response to abiotic stressors are mismatched in low diversity edge populations. *J. Ecol.* **97**, 450–462. (doi:10.1111/j.1365-2745.2009.01481.x)
71. Miller AD, Coleman MA, Clark J, Cook R, Naga Z, Doblin MA, Hoffmann AA, Sherman CD, Bellgrove A. 2020 Local thermal adaptation and limited gene flow constrain future climate responses of a marine ecosystem engineer. *Evol. Appl.* **13**, 918–934. (doi:10.1111/eva.12909)
72. McCoy SJ, Widdicombe S. 2019 Thermal plasticity is independent of environmental history in an intertidal seaweed. *Ecol. Evol.* **9**, 13 402–13 412. (doi:10.1002/ece3.5796)
73. Liesner D, Shama LNS, Diehl N, Valentin K, Bartsch I. 2020 Thermal plasticity of the kelp *Laminaria digitata* (Phaeophyceae) across life cycle stages reveals the importance of cold seasons for marine forests. *Front. Mar. Sci.* **7**, 456. (doi:10.3389/fmars.2020.00456)
74. Veenhof RJ, Champion C, Dworjanyn SA, Schwoerbel J, Visch W, Coleman MA. 2023 Projecting kelp (*Ecklonia radiata*) gametophyte thermal adaptation and persistence under climate change. *Ann. Bot.* mcad132. (doi:10.1093/aob/mcad132)
75. Coleman MA, Roughan M, Macdonald HS, Connell SD, Gillanders BM, Kelaher BP, Steinberg PD. 2011 Variation in the strength of continental boundary currents determines continent-wide connectivity in kelp. *J. Ecol.* **99**, 1026–1032. (doi:10.1111/j.1365-2745.2011.01822.x)
76. Tatsumi M, Layton C, Cameron MJ, Shelamoff V, Johnson CR, Wright JT. 2021 Interactive effects of canopy-driven changes in light, scour and water flow on microscopic recruits in kelp. *Mar. Environ. Res.* **171**, 105450. (doi:10.1016/j.marenvres.2021.105450)
77. Tatsumi M, Mabin CJT, Layton C, Shelamoff V, Cameron MJ, Johnson CR, Wright JT. 2022 Density-dependence and seasonal variation in reproductive output and sporophyte production in the kelp, *Ecklonia radiata*. *J. Phycol.* **58**, 92–104. (doi:10.1111/jpy.13214)
78. Schiel DR, Foster MS. 2006 The population biology of large brown seaweeds: ecological consequences of multiphase life histories in dynamic coastal environments. *Ann. Rev. Ecol. Evo. Syst.* **37**, 343–372. (doi:10.1146/annurev.ecolsys.37.091305.110251)
79. Kirkman H. 1984 Standing stock and production of *Ecklonia radiata* (C.Ag.): J. Agardh. *J. Exp. Mar. Biol. Ecol.* **76**, 119–130.
80. Layton C , Shelamoff V, Cameron MJ, Tatsumi M, Wright JT, Johnson CR. 2019 Resilience and stability of kelp forests: the importance of patch dynamics and environment-engineer feedbacks. *PLoS ONE* **14**, e0210220.
81. Mabin CJT, Gribben PE, Fischer A, Wright JT. 2013 Variation in the morphology, reproduction and development of the habitat-forming kelp *Ecklonia radiata* with changing temperature and nutrients. *Mar. Ecol. Prog. Ser.* **483**, 117–131.
82. Biancacci C *et al.* 2022 Optimisation of at-sea culture and harvest conditions for cultivated *Macrocystis pyrifera*: yield, biofouling and biochemical composition of cultured biomass. *Front. Mar. Sci.* **9**, 951538. (doi:10.3389/fmars.2022.951538)
83. EgerAM, Layton C, McHugh T, Gleason M, Eddy N. 2022 *Kelp restoration guidebook: lessons learned from kelp projects around the world*. Arlington, TX: The Nature Conservancy.
84. Frölicher TL, Fischer EM, Gruber N. 2018 Marine heatwaves under global warming. *Nature* **560**, 360–364. (doi:10.1038/s41586-018-0383-9)
85. Oliver ECJ, Lago V, Hobday AJ, Holbrook NJ, Ling SD, Mundy CN. 2018 Marine heatwaves off eastern Tasmania: trends, interannual variability, and predictability. *Prog. Oceanogr.* **161**, 116–130. (doi:10.1016/j.pocean.2018.02.007)
86. Buschmann AH, Moreno C, Vásquez JA, Hernández-González MC. 2006 Reproduction strategies of *Macrocystis pyrifera* (Phaeophyta) in Southern Chile: the importance of population dynamics. *J. Appl. Phycol.* **18**, 575. (doi:10.1007/s10811-006-9063-5)
87. Britton D, Layton C, Mundy CN, Brewer EA, Gaitán-Espitia JD, Beardall J, Raven JA, Hurd CL. 2024 Cool-edge populations of the kelp *Ecklonia radiata* under global ocean change scenarios: strong sensitivity to ocean warming but little effect of ocean acidification. Figshare. (doi:10.6084/m9.figshare.c.6991797)